Interactions of Gold Nanoparticles with a Phospholipid Monolayer Membrane on Mercury

Gabriel J. Gordillo,[†,*] Željka Krpetić,[‡,§] and Mathias Brust[‡,*]

[†]Departamento de Química Inorgánica, Analítica y Química Física, Facultad de Ciencias Exactas y Naturales, INQUIMAE (CONICET), Universidad de Buenos Aires, Ciudad Universitaria, Pabellón 2, 1428, Buenos Aires, Argentina and [‡]Department of Chemistry, University of Liverpool, Crown Street, Liverpool L69 7ZD, United Kingdom [§]Present address: Dr. Željka Krpetić, Centre for BioNano Interactions, School of Chemistry and Chemical Biology, University College Dublin, Belfield, Dublin 4, Ireland.

ABSTRACT It is demonstrated that a compact monolayer of 1,2-dioleoyl-*sn*-glycero-3-phosphocholine adsorbed to a hanging mercury drop electrode can serve as a simple electrochemical model system to study biomembrane penetration by gold nanoparticles. The hydrogen redox-chemistry characteristic of ligand-stabilized gold nanoparticles in molecularly close contact with a mercury electrode is used as an indicator of membrane penetration. Results for water-dispersible gold nanoparticles of two different sizes are reported, and comparisons are made with the cellular uptake of the same preparations of nanoparticles by a common human fibroblast cell line. The experimental system described here can be used to study physicochemical aspects of membrane penetration in the absence of complex biological mechanisms, and it could also be a starting point for the development of a test bed for the toxicity of nanomaterials.

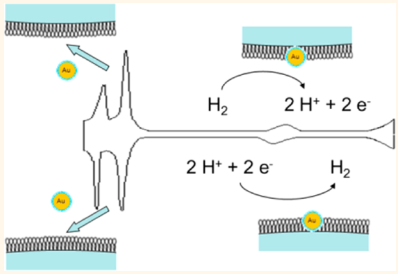

KEYWORDS: gold nanoparticles · phospholipid monolayer · electrochemistry · membrane penetration · mercury electrode · nanotoxicology

All biological cells are surrounded by a phospholipid bilayer membrane, which represents a robust barrier to most molecules and all ions and allows the cell to maintain conditions inside that are very different from those in the extracellular medium.[1] In general, only small neutral molecules such as oxygen, carbon dioxide, and water can freely diffuse across the membrane and rapidly establish their equilibrium concentrations on both sides.[2,3] Given the need for living cells to regularly exchange matter with their environment, in addition to this barrier function, the cell membrane also needs to selectively allow or enable the transport of material in both directions. This is achieved by a host of specific carrier proteins and ion channels and by a number of different mechanisms of endo- and exocytosis.[4] The general paradigm that macromolecules and nanoscopic objects can enter cells exclusively *via* endocytosis is increasingly being challenged by growing experimental and computational evidence of uptake that circumvents endocytic mechanisms and implies the existence of mechanisms of direct membrane penetration by nanoparticles.[5−12] Such direct uptake, if further substantiated, may become relevant to drug delivery, incorporation of intracellular probes, some viral infections, transfection in general, protein trafficking, and toxicity studies of both natural and artificial nanoscale objects. The latter, in particular, is very topical since the current implementation of nanoparticles in a broad range of applied technologies is expected to cause a significant increase in the exposure of humans and the environment to such materials.[13,14] The simplest initial criterion of whether a nanoparticle is toxic or not may indeed be whether or not it finds a way to overcome the barrier function of the cell membrane.[15] Experimental test beds for such scenarios may hence become of some practical importance for the health and safety assessment of nanomaterials. Recently, cell-penetrating peptides (CPPs) have been discussed extensively as agents that can enable the direct uptake of an attached payload that could be genetic material, a protein, or a nanoparticle.[5,7,9,12,16−18] While

* Address correspondence to gabriel@qi.fcen.uba.ar; M.Brust@liv.ac.uk.

Received for review March 11, 2014 and accepted May 30, 2014.

Published online May 30, 2014
10.1021/nn501395e

some experimental evidence suggests the absence of an endocytic mechanism, the possibility of direct membrane transfer by CPP-modified objects is still subject to debate.[18] Some of us recently reported that CPP-modified gold nanoparticles readily negotiate intracellular membrane boundaries; for example, they escape into the cytosol from vesicular structures.[9] Additional evidence of direct membrane penetration by nanoscopic objects comes from electron microscopic studies of the cellular uptake of various artificial nanoparticles.[5,7,9,11,12,16−18] While in most cases, as expected, endocytosis and subsequent localization of the material in endocytic vesicles is observed as the only route,[12] some reports clearly show nanoparticles freely dispersed in the cytosol, indicating an uptake mechanism other than endocytosis.[7,9,11,19,20] Although, it is possible to deliberately block endocytosis[21,22] and thus limit the range of potential uptake routes, when studying live cells it remains difficult to distinguish between simple physicochemical effects and the more complex biological response mechanisms.[23] For this reason, we have revived a relatively old and well-established model system that should allow us to readily monitor membrane penetration by nanoparticles in the guaranteed absence of biological uptake mechanisms. Our system of choice is a monolayer of the phospholipid 1,2-dioleoyl-*sn*-glycero-3-phosphocholine (DOPC) adsorbed to the surface of a hanging mercury drop electrode (HMDE).[24] In the past, this simple model of "half a bilayer membrane" has been particularly useful to study the electrochemistry of membrane-bound redox couples that play important roles in nature, for example in the respiratory chain.[25,26] Recently, Nelson and co-workers have also applied this system successfully to study the size dependence of nanoparticle/membrane interactions and to image and monitor the formation of adsorbed layers of silica particles.[27,28] A benefit of this model membrane demonstrated in the present contribution is that an immediate, strong, and characteristic electrochemical signal is obtained as soon as gold nanoparticles penetrate the monolayer and establish electrical contact with the mercury surface. Free-standing model membranes, in comparison, show quite subtle differences in membrane capacitance between nanoparticle adsorption and penetration.[29]

RESULTS AND DISCUSSION

The experimental system chosen here to interrogate membrane penetration by gold nanoparticles is shown in Figure 1. The surface of a hanging mercury drop working electrode is covered by a passivating DOPC monolayer layer, which prevents gold particles suspended in the electrolyte solution from making electrical contact with the electrode unless the particles penetrate the DOPC monolayer. Phospholipid monolayers of this type have been extensively studied in the past and are readily assembled by carefully passing the

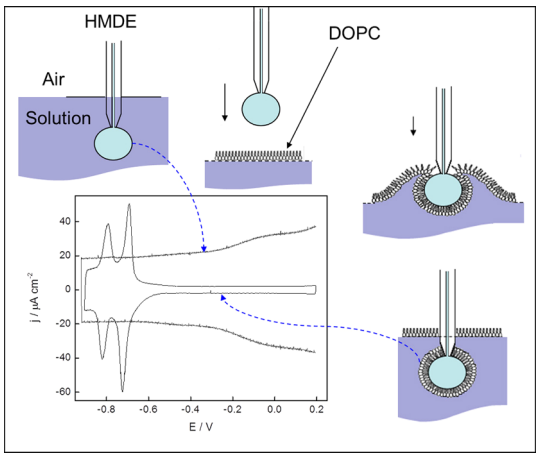

Figure 1. Schematic representation of DOPC monolayer formation on a hanging mercury drop electrode (HMDE). The monolayer is formed by carefully passing the electrode through a compact DOPC layer at the water/air interface obtained by spreading and evaporating a controlled amount of the phospholipid dissolved in pentane. Note the significant drop in capacitance and the appearance of the characteristic reorganization peaks in the cyclic voltammogram after formation of the monolayer (potential sweep rate: 1 V s^{-1}).

mercury drop electrode through a monolayer of the phospholipid on the surface of the electrolyte solution.[24−26,30] This is obtained by spreading and evaporating a set amount of the lipid dissolved in pentane (typically 4 μL of a 0.25 mM solution of DOPC in pentane is spread per cm^2 surface area to be covered). The ability to detect an electrochemical signal associated with particle penetration is closely related to our previously reported finding of reversible electrocatalytic hydrogen ion reduction on gold nanoparticles adsorbed to a clean hanging mercury drop electrode.[31] There, it was shown that ligand-protected gold nanoparticles identical to those used in the present study adsorb spontaneously to the mercury surface and act as stable electrocatalytic reaction centers without leading to amalgam formation even after many hours of contact with mercury. The characteristic redox peak observed when the gold nanoparticles are in contact with the mercury electrode is attributed, for the cathodic sweep, to the sequential two-electron-transfer reduction of protons to form adsorbed hydrogen on the nanoparticle surface, and, for the anodic sweep, to the corresponding desorptive oxidation of dihydrogen. In the present system, a similar electrochemical signal should be observed when the particles penetrate the DOPC monolayer and make contact with the mercury. The results of our study using PEGylated gold nanoparticles of *ca.* 10 nm diameter are presented in Figure 2. In the potential range between 0 and -0.3 V *versus* SHE only capacitive charging of the monolayer-covered electrode is observed, indicating that the gold nanoparticles present in the electrolyte do not establish electrical contact with the electrode; that is, the membrane acts as an efficient barrier for these

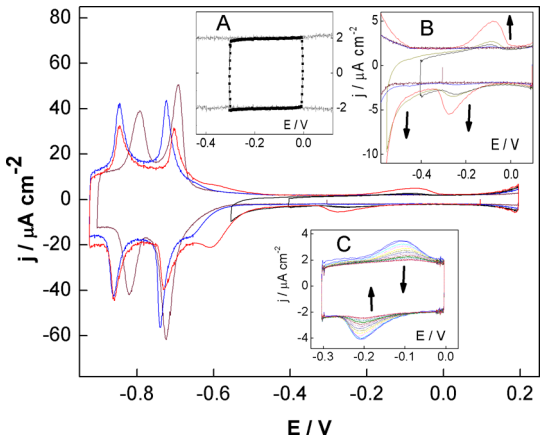

Figure 2. Insertion of 10 nm gold nanoparticles into the DOPC monolayer occurs only when the potential sweep is extended into the reorganization region negative of −0.7 V. The main figure shows the full-range cyclic voltammogram in the absence of nanoparticles (brown) and the first (blue) and second (red) sweep into the reorganization region in the presence of nanoparticles (potential sweep rate: 1 V s^{-1}). Note that the peaks characteristic of hydrogen redox chemistry on gold nanoparticles appear as soon as the potential sweep includes the reorganization region; that is, they are present in the second consecutive sweep into this region. We attribute this to electroporation of the monolayer in the reorganization region. Note also that the presence of nanoparticles alters the properties of the DOPC monolayer, which is manifested in changes in position and appearance of the reorganization peaks. Inset A: Cycling the potential in the 0 to −0.3 V range in the presence of 10 nm gold particles prior to expanding the potential sweep into the reorganization region. From the absence of an electrochemically active species it is concluded that the particles do not penetrate the DOPC monolayer under these conditions. Inset B: Magnification of a feature from the main figure showing the appearance and increase of the hydrogen redox peak due to insertion of gold nanoparticles upon repeated potential cycling into the reorganization region, first cycle blue, second red. The green and subsequently the gray line show that this peak gradually disappears again as soon as the potential sweeps are restricted to a potential range in which the monolayer is compact. This is shown in more detail in inset C. Inset C: Gradual decline of the hydrogen redox peaks observed over 50 successive potential cycles between 0 and −0.3 V. This indicates the expulsion of nanoparticles from the DOPC layer.

particles in the potential range indicated. This changes dramatically as soon as the potential sweep is extended to range from 0.1 to −1 V *versus* SHE, where the DOPC monolayer undergoes a reorganization associated with a pair of well-established sharp capacitive charging peaks. These reorganization peaks are shown in Figure 2 initially in the absence of gold nanoparticles. When gold nanoparticles are added, following the first excursion into this potential range, the characteristic reversible peak due to adsorptive hydrogen ion reduction on the gold nanoparticles appears on the subsequent potential sweep, indicating insertion of gold nanoparticles into the lipid monolayer. This peak increases gradually with subsequent scans. The reorganization peaks also change in appearance when gold nanoparticles are integrated in the membrane, indicating that this process affects the general properties of the monolayer membrane. Given the relatively low concentration of gold nanoparticles in the electrolyte solution, their immediate detection in the cyclic voltammogram can be explained only by the prior adsorption of a layer of nanoparticles to the phospholipid monolayer. This is in accordance with previously reported membrane adsorptive behavior of nanoparticles capable of adopting a certain degree of amphiphilicity.[11,29,32,33]

We interpret the reorganization peaks at negative potentials as a reversible electroporation of the DOPC layer. This is also supported by previous observations.[30,34]

As soon as the pores are formed, the gold nanoparticles adsorbed to the DOPC-modified electrode surface are integrated into the layer and exhibit their characteristic electrochemical feature (Figure 2). More particles insert into the monolayer with further potential scans. However, if subsequently the electroporation potential is again avoided, the peaks that are due to the insertion of gold nanoparticles gradually disappear, which we interpret as expulsion of the gold nanoparticles and reannealing of the DOPC monolayer. These observations are a robust indication of the integrity of the layer over a broad potential range and its efficient barrier function against the spontaneous insertion of the 10 nm gold particles.

An alternative explanation to the temporary opening of pores in the DOPC layer is its mechanical expansion that may be caused, for example, by a slight increase in the size of the mercury drop at negative potentials. To make sure this effect was avoided, the lipid reorganization peak at −0.725 V (Figure 1) was used as an internal reference indicating the presence of a complete surface coverage ($\theta = 1$). Nelson and Benton have demonstrated the strong dependence of the height of this peak on surface coverage.[24] As mentioned before, heights of the first reorientation peaks corresponding to 55 ± 5 μF cm^{-2} allowed us to ensure the quality and integrity of the monolayer in all experiments.

Our study, so far, concludes that 10 nm PEGylated gold nanoparticles cannot spontaneously penetrate the DOPC monolayer. This is congruent with observations in cell cultures, where uptake of such particles is either not observed or limited to a biological endocytosis process that does not involve the direct penetration of the plasma membrane.[7,9]

A completely different scenario is observed for much smaller, 2−3 nm gold nanoparticles of the same PEG/thiol surface chemistry. As shown in Figure 3, these particles, as soon as they are added to the electrolyte solution, start penetrating the phospholipid monolayer, which is manifested in the steadily increasing reversible redox peak at −0.2 V due to the previously described characteristic hydrogen redox chemistry on gold nanoparticles in contact with the mercury electrode.[31]

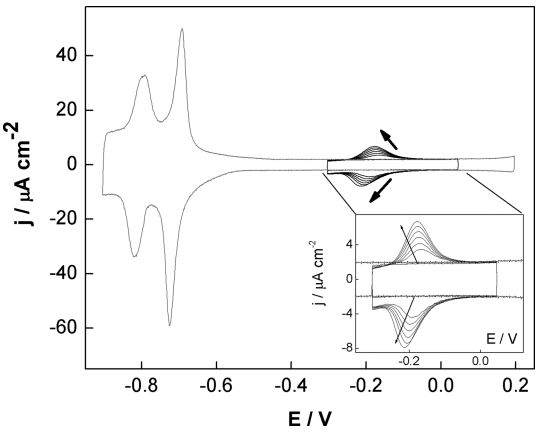

Figure 3. Spontaneous penetration of the compact DOPC monolayer by 2 nm gold nanoparticles. The cyclic voltammogram of the DOPC monolayer over the full potential range is shown only for reference since in this experiment the electrode potential was limited at all times to the 0.05 to −0.3 V range. The inset shows in detail the gradual development of the characteristic hydrogen redox peaks, indicating continuing insertion of nanoparticles into the DOPC monolayer. Note that this happens while the DOPC monolayer remains compact at all times as the potential is never close to the reorganization region. Over prolonged exposure to the nanoparticles the electrode capacitance gradually increases, and eventually the DOPC monolayer is completely replaced by a monolayer of adsorbed nanoparticles.

Depending on their concentration and on the time scale of the experiment, the electrochemical features characteristic of a compact DOPC monolayer eventually disappear, and the hydrogen redox peaks remain as the only salient feature in the cyclic voltammogram, suggesting that the nanoparticles can fully replace the phospholipid monolayer to form an adsorbed monolayer themselves. This contrasts the behavior of the larger particles, which did not penetrate the compact monolayer and, when integrated by electroporation, were expelled again at more positive potentials. The nanoparticles and the DOPC can thus simply be regarded as two different surfactants in competition for the same interface. While the larger particles are cleared from the interface by the DOPC, the smaller ones are capable of competing with the DOPC and eventually replace it from the interface.

Our study also reveals quantitatively the electrode surface coverage with nanoparticles inserted into the DOPC monolayer, as well as some insertion and expulsion rates. In a previous paper we have demonstrated that the charge per unit electrode area, Q_s, corresponding to the electrochemical redox process associated with the presence of the gold nanoparticle film in the absence of a lipid monolayer, was the same for two different particle diameters studied (in that case 14 and 2 nm): $Q_s = 17 \pm 1\ \mu C\ cm^{-2}$.

In the present case, the charge transferred when the maximum observed number of 10 nm gold nanoparticles were inserted in the DOPC monolayer (Figure 2) was $Q_{np} = 0.36\ \mu C\ cm^{-2}$. This corresponds to coverage of 8.6×10^9 nanoparticles per cm^2. Assuming that the access of protons to the particles' surface is not significantly restricted by the presence of the DOPC monolayer, the area ratio Q_{np}/Q_s allows estimating that under these conditions *ca.* 2% of the electrode area was covered by nanoparticles. The inset C of Figure 2 shows the expulsion of the 10 nm particles from the DOPC monolayer while the potential was cycled between 0 and −0.3 V. In this case, starting from a coverage of $Q_{np} = 0.17\ \mu C\ cm^{-2}$ (4×10^9 nanoparticles per cm^2), the expulsion rate at the beginning of the experiment is $V_{d,q} = 3$ nC/s or $V_{d,nps} = 7.3 \times 10^7$ NPs/s (see also Supporting Information, SI). The inset of Figure 3 shows the insertion of 2 nm particles while the potential is cycled between 0.1 and −0.3 V. In this case, the insertion rate at the beginning of the experiment is $V_{ad,q} = 45.6$ nC/s or $V_{ad,nps} = 1.9 \times 10^{10}$ NPs/s.

To what extent our observations are translatable to a biological environment can of course be assessed only once the behavior of a number of different nanoparticles in model systems of the type described here has been compared with that in biological scenarios. As a first step in this direction, we have compared the cellular uptake of both the large and the small nanoparticles by HeLa cells, a common human fibroblast cell line. For this purpose, we have carried out three separate experiments: incubation of cell cultures (i) with 10 nm particles, (ii) with 2−3 nm particles, and (iii) with a mixture of 10 and 2−3 nm particles, all followed by inspection of the cells by TEM. In all cases, in line with the predictions from our model system, uptake was observed only for the small particles. Unfortunately, these are so small that their unambiguous identification inside cells based on TEM images alone requires careful and unbiased inspection of a large number of images. For this reason, additional representative images are provided in the SI. It is worth mentioning here that Eychmüller and co-workers have reported the spontaneous penetration of model and biological cell membranes by CdTe quantum dots of similar size and surface modification.[11] Our findings are in agreement with theirs. The images in Figure 4 show many of the small particles enclosed in vesicles, which is indicative of uptake by endocytosis, a process not predictable by our simple model. On the other hand, the particles are also found freely dispersed in the cytoplasm (see SI) and in the inner and outer mitochondrial membrane, both indicative of their membrane-penetrating properties. Note, there are no mitochondrial uptake mechanisms for objects of this size that are not proteins. Although more comparative work is needed to validate the monolayer model membrane as a predictive tool for the penetration of real biomembranes by nanoparticles, our preliminary results suggest that there is a correlation. What has not been considered here are the effects of microscopic heterogeneities and the presence of proteins and

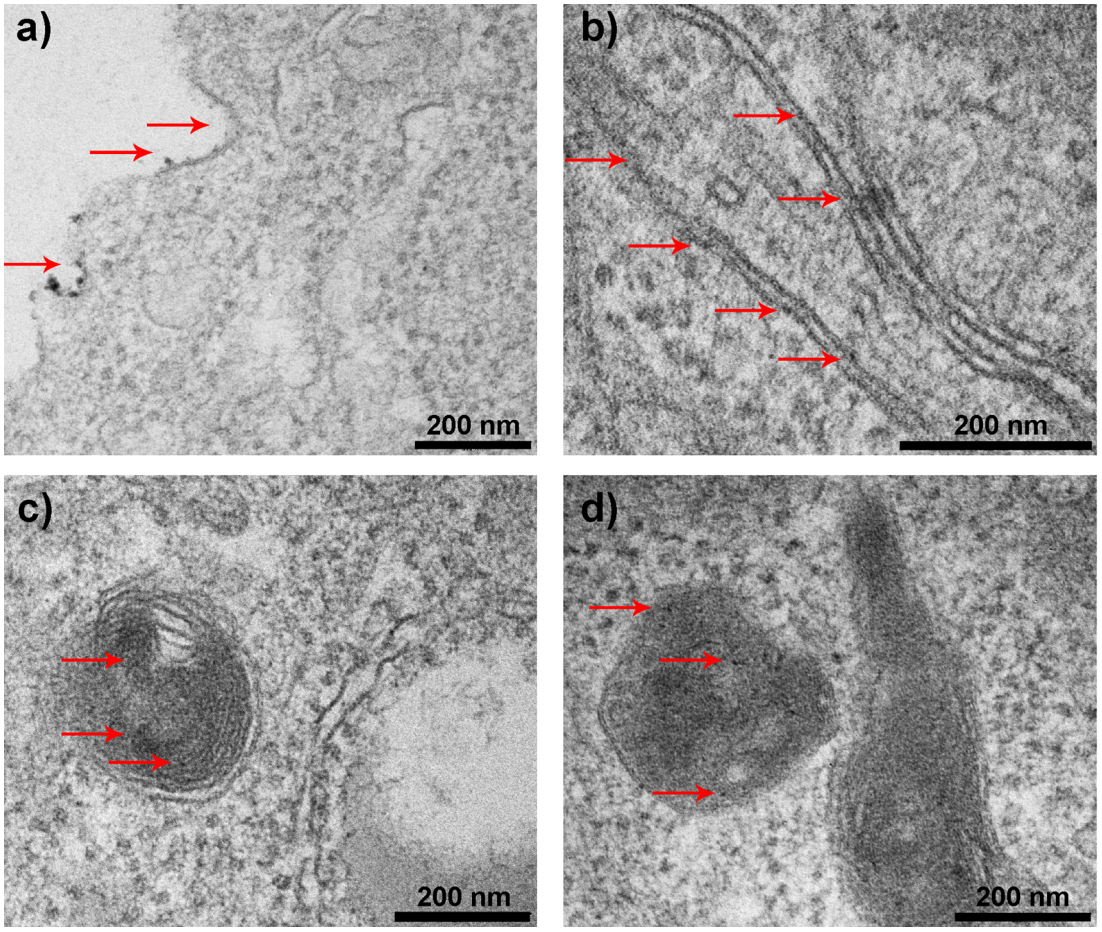

Figure 4. TEM micrographs of GNPs in HeLa cells. Red arrows point to (a) small-sized gold nanoparticles/nanoparticle clusters present at the cell membrane; (b) small-sized nanoparticles present in the mitochondrial membrane of HeLa cells; (c) nanoparticles present in the multivesicular bodies in the cell cytoplasm; and (d) nanoparticles present in the lysosomes of HeLa cells.

charged domains, which are all important in determining the properties of biological cell membranes. These limitations notwithstanding, the model introduced should predict the penetration of biomembranes by nanoparticles as long as this is chiefly governed by general physicochemical parameters and not by specific recognition or other more complex biochemical mechanisms.

CONCLUSIONS

It has been demonstrated that the ability of gold nanoparticles to spontaneously penetrate biological membranes can be evaluated using an established electrochemical membrane model. Preliminary findings of a comparative cellular uptake study with a standard human cell line indicate that the results obtained from the electrochemical model are relevant to the behavior of the particles in the biological system. Larger particles that were unable to penetrate compact monolayers in the model system were also unable to cross the biological cell membrane, while smaller particles readily transferred across both membrane systems. Model systems such as the one described here may play a future role in standardizing the toxicological evaluation of nanomaterials and in designing new physicochemical cellular entry mechanisms for drug delivery across biological boundaries. From a more fundamental point of view, such systems represent fascinating experimental models that enable studies of nanoscale self-organization and electron transfer processes involving carefully selected biological and nonbiological components.

MATERIALS AND METHODS

Gold Nanoparticles. The preparation of gold nanoparticles of 2–3 and of 10 nm diameter, both ligand-stabilized, *i.e.*, PEGylated, by 1-mercaptoundecane-11-tetra(ethylene glycol), has recently been described elsewhere.[31] The protocols followed established literature methods.[35–37] For details on the preparation and characterization of the nanoparticles by UV–vis spectroscopy and differential centrifugal sedimentation[38] see the SI.

Electrochemistry. Cyclic voltammetry was carried out using a standard electrochemical cell with an HMDE working electrode

(Beckman), a Pt wire counter electrode, and an Ag/AgCl (KCl 3.5 M) reference electrode. All potentials are quoted *versus* the standard hydrogen electrode (SHE). The potential was controlled with a TEQ potentiostat (Argentina). All electrolyte solutions used were 0.2 M sodium acetate/acetic acid buffer at pH 4.8. The molar concentration of all gold nanoparticle dispersions used in electrochemical experiments was 2 nM. The potential sweep rate in all experiments reported was 1 V s^{-1}.

HMDE Modified with DOPC Monolayer. The experimental details for the preparation of the phospholipid membrane have been described in detail elsewhere.[24] Briefly, a solution of DOPC in pentane was spread and allowed to evaporate on the surface of the electrolyte solution, leaving behind a monolayer of DOPC. To obtain a DOPC monolayer on the electrode surface, the HMDE was carefully pushed once through the water/air interface from outside the electrolyte solution. The quality of the monolayer was judged from the appearance of the cyclic voltammogram (see Figure 1) and by ensuring that the height of the first orientation peaks at −0.725 V corresponded to 55 ± 5 μF cm^{-2} (equivalent to a peak current density of 55 μA cm^{-2} at a potential sweep rate of 1 V s^{-1}).

Conflict of Interest: The authors declare no competing financial interest.

Supporting Information Available: Materials: S1. Preparation and functionalization of gold nanoparticles; S2. Characterization of gold nanoparticles; S3. Transmission electron microscopy (TEM) of biological samples; S4. Gallery of representative TEM images. S5. Electrochemistry. This material is available free of charge *via* the Internet at http://pubs.acs.org.

Acknowledgment. G.G. and M.B. are grateful recipients of a Royal Society Joint Project Grant. G.G. (member of the National Research Council of Argentina-CONICET) also acknowledges financial support from UBACYT (Proy. 0278). M.B. is recipient of an ERC Advanced Grant (PANDORA). Z.K. was partially supported by the EU Framework Project BisNano, thus acknowledging the European Union Seventh Framework Program (FP7/2007-2013) under grant agreement no. 263878.

REFERENCES AND NOTES

1. van Meer, G.; Voelker, D. R.; Feigenson, G. W. Membrane Lipids: Where They are and How They Behave. *Nat. Rev. Mol. Cell. Biol.* **2008**, *9*, 112–124.
2. Colvin, V. L. The Potential Environmental Impact of Engineered Nanomaterials. *Nat. Biotechnol.* **2003**, *21*, 1166–1170.
3. Donaldson, K.; Stone, V.; Tran, C. L.; Kreyling, W.; Borm, P. J. Nanotoxicology. *Occup. Environ. Med.* **2004**, *61*, 727–728.
4. Conner, S. D.; Schmid, S. L. Regulated Portals of Entry into the Cell. *Nature* **2003**, *422*, 37–44.
5. de la Fuente, J. M.; Berry, C. C. Tat Peptide as an Efficient Molecule To Translocate Gold Nanoparticles into the Cell Nucleus. *Bioconjugate Chem.* **2005**, *16*, 1176–1180.
6. Verma, A.; Uzun, O.; Hu, Y.; Hu, Y.; Han, H.-S.; Watson, N.; Chen, S.; Irvine, D. J.; Stellacci, F. Surface-Structure-Regulated Cell-Membrane Penetration by Monolayer-Protected Nanoparticles. *Nat. Mater.* **2008**, *7*, 588–595.
7. Nativo, P.; Prior, I. A.; Brust, M. Uptake and Intracellular Fate of Surface-Modified Gold Nanoparticles. *ACS Nano* **2008**, *2*, 1639–1644.
8. Lin, J.; Zhang, H.; Chen, Z.; Zheng, Y. Penetration of Lipid Membranes by Gold Nanoparticles: Insights into Cellular Uptake, Cytotoxicity, and Their Relationship. *ACS Nano* **2010**, *4*, 5421–5429.
9. Krpetic, Z.; Saleemi, S.; Prior, I. A.; See, V.; Qureshi, R.; Brust, M. Negotiation of Intracellular Membrane Barriers by TAT-Modified Gold Nanoparticles. *ACS Nano* **2011**, *5*, 5195–5201.
10. Cioran, A. M.; Musteti, A. D.; Teixidor, F.; Krpetic, Z.; Prior, I. A.; He, Q.; Kiely, C. J.; Brust, M.; Vinas, C. Mercaptocarborane-Capped Gold Nanoparticles: Electron Pools and Ion Traps with Switchable Hydrophilicity. *J. Am. Chem. Soc.* **2012**, *134*, 212–221.
11. Dubavik, A.; Sezgin, E.; Lesnyak, V.; Gaponik, N.; Schwille, P.; Eychmüller, A. Penetration of Amphiphilic Quantum Dots through Model and Cellular Plasma Membranes. *ACS Nano* **2012**, *6*, 2150–2156.
12. Salvati, A.; Pitek, A. S.; Monopoli, M. P.; Prapainop, K.; Bombelli, F. B.; Hristov, D. R.; Kelly, P. M.; Aberg, C.; Mahon, E.; Dawson, K. A. Transferrin-Functionalized Nanoparticles Lose Their Targeting Capabilities When a Biomolecule Corona Adsorbs on the Surface. *Nat. Nanotechnol.* **2013**, *8*, 137–146.
13. Stone, V.; Donaldson, K. Nanotoxicology: Signs of Stress. *Nat. Nanotechnol.* **2006**, *1*, 23–24.
14. Dawson, K. A.; Salvati, A.; Lynch, I. Nanotoxicology: Nanoparticles Reconstruct Lipids. *Nat. Nanotechnol.* **2009**, *4*, 84–85.
15. Kim, S. T.; Saha, K.; Kim, C.; Rotello, V. M. The Role of Surface Functionality in Determining Nanoparticle Cytotoxicity. *Acc. Chem. Res.* **2013**, *46*, 681–691.
16. Brooks, N. A.; Pouniotis, D. S.; Tang, C. K.; Apostolopoulos, V.; Pietersz, G. A. Cell-Penetrating Peptides: Application in Vaccine Delivery. *BBA-Rev. Cancer* **2010**, *1805*, 25–34.
17. Johnson, R. M.; Harrison, S. D.; Maclean, D. Therapeutic Applications of Cell-Penetrating Peptides. *Methods Mol. Biol.* **2011**, *683*, 535–551.
18. Koren, E.; Torchilin, V. P. Cell-Penetrating Peptides: Breaking through to the Other Side. *Trends Mol. Med.* **2012**, *18*, 385–393.
19. Gao, H.; Yang, Z.; Zhang, S.; Cao, S.; Shen, S.; Pang, Z.; Jiang, X. Ligand Modified Nanoparticles Increases Cell Uptake, Alters Endocytosis and Elevates Glioma Distribution and Internalization. *Sci. Rep.* **2013**, *3*, 2534:1–8.
20. Saha, K.; Kim, S. T.; Yan, B.; Miranda, O. R.; Alfonso, F. S.; Shlosman, D.; Rotello, V. M. Surface Functionality of Nanoparticles Determines Cellular Uptake Mechanisms in Mammalian Cells. *Small* **2013**, *9*, 300–305.
21. Punnonen, E. L.; Ryhanen, K.; Marjomaki, V. S. At Reduced Temperature, Endocytic Membrane Traffic Is Blocked in Multivesicular Carrier Endosomes in Rat Cardiac Myocytes. *Eur. J. Cell. Biol.* **1998**, *75*, 344–352.
22. Kirchhausen, T.; Macia, E.; Pelish, H. E. Use of Dynasore, the Small Molecule Inhibitor of Dynamin, in the Regulation of Endocytosis. *Methods Enzymol.* **2008**, *438*, 77–93.
23. Monopoli, M. P.; Aberg, C.; Salvati, A.; Dawson, K. A. Biomolecular Coronas Provide the Biological Identity of Nanosized Materials. *Nat. Nanotechnol.* **2012**, *7*, 779–786.
24. Nelson, A.; Benton, A. Phospholipid Monolayers at the Mercury/Water Interface. *J. Electroanal. Chem. Interfacial Electrochem.* **1986**, *202*, 253–270.
25. Gordillo, G. J.; Schiffrin, D. J. The Electrochemistry of Ubiquinone-10 in a Phospholipid Model Membrane. *Faraday Discuss.* **2000**, *116*, 89–107.
26. Moncelli, M. R.; Becucci, L.; Nelson, A.; Guidelli, R. Electrochemical Modeling of Electron and Proton Transfer to Ubiquinone-10 in a Self-Assembled Phospholipid Monolayer. *Biophys. J.* **1996**, *70*, 2716–2726.
27. Zhang, S.; Nelson, A.; Beales, P. A. Freezing or Wrapping: The Role of Particle Size in the Mechanism of Nanoparticle–Biomembrane Interaction. *Langmuir* **2012**, *28*, 12831–12837.
28. Vakurov, A.; Brydson, R.; Nelson, A. Electrochemical Modeling of the Silica Nanoparticle–Biomembrane Interaction. *Langmuir* **2011**, *28*, 1246–1255.
29. Carney, R. P.; Astier, Y.; Carney, T. M.; Voïtchovsky, K.; Jacob Silva, P. H.; Stellacci, F. Electrical Method to Quantify Nanoparticle Interaction with Lipid Bilayers. *ACS Nano* **2012**, *7*, 932–942.
30. Almaleck, H.; Gordillo, G. J.; Disalvo, A. Water Defects Induced by Expansion and Electrical Fields in DMPC and DMPE Monolayers: Contribution of Hydration and Confined Water. *Colloids Surf., B* **2013**, *102*, 871–878.
31. Brust, M.; Gordillo, G. J. Electrocatalytic Hydrogen Redox Chemistry on Gold Nanoparticles. *J. Am. Chem. Soc.* **2012**, *134*, 3318–3321.
32. Dubavik, A.; Lesnyak, V.; Gaponik, N.; Eychmüller, A. One-Phase Synthesis of Gold Nanoparticles with Varied Solubility. *Langmuir* **2011**, *27*, 10224–10227.

33. Tatur, S.; Maccarini, M.; Barker, R.; Nelson, A.; Fragneto, G. Effect of Functionalized Gold Nanoparticles on Floating Lipid Bilayers. *Langmuir* **2013**, *29*, 6606–6614.
34. Nelson, A. Electrochemistry of Mercury Supported Phospholipid Monolayers and Bilayers. *Curr. Opin. Colloid Interface Sci.* **2010**, *15*, 455–466.
35. Turkevich, J.; Stevenson, P. C.; Hillier, J. A Study of the Nucleation and Growth Processes in the Synthesis of Colloidal Gold. *Discuss. Faraday Soc.* **1951**, *11*, 55–75.
36. Frens, G. Controlled Nucleation for Regulation of Particle-Size in Monodisperse Gold Suspensions. *Nat. Phys. Sci.* **1973**, *241*, 20–22.
37. Brust, M.; Walker, M.; Bethell, D.; Schiffrin, D. J.; Whyman, R. Synthesis of Thiol-Derivatised Gold Nanoparticles in a Two-Phase Liquid-Liquid System. *J. Chem. Soc., Chem. Commun.* **1994**, 801–802.
38. Krpetic, Z.; Davidson, A. M.; Volk, M.; Levy, R.; Brust, M.; Cooper, A. I. High Resolution Sizing of Monolayer Protected Gold Clusters by Differential Centrifugal Sedimentation. *ACS Nano* **2013**, *7*, 8881–8890.